Available online at www.sciencedirect.com
SciVerse ScienceDirect
Ceramics International 38 (2012) 6359–6363
CERAMICS INTERNATIONAL
www.elsevier.com/locate/ceramint

High piezoelectric coefficient of Pr_2O_3-doped $Ba_{0.85}Ca_{0.15}Ti_{0.90}Zr_{0.10}O_3$ ceramics

Chao Han[a], Jiagang Wu[a,*], Chaohui Pu[b], Sha Qiao[a], Bo Wu[a], Jianguo Zhu[a], Dingquan Xiao[a]

[a]*Department of Materials Science, Sichuan University, Chengdu 610064, PR China*
[b]*Shanghai Institute of Microsystem and Information Technology, Chinese Academy of Sciences, Shanghai 200050, PR China*

Received 28 April 2012; received in revised form 3 May 2012; accepted 3 May 2012
Available online 11 May 2012

Abstract

Pr_2O_3-doped $Ba_{0.85}Ca_{0.15}Ti_{0.90}Zr_{0.10}O_3$ (BCTZ-*x*Pr) ceramics were prepared by the conventional solid-state method. A tetragonal phase is only observed in these ceramics, and the introduction of Pr_2O_3 decreases their sintering temperature without affecting negatively the piezoelectric constant. Enhanced ferroelectric properties were obtained in these BCTZ-*x*Pr ceramics. The ceramic with $x=0.06$ wt% exhibits a good electrical behavior of $d_{33}\sim460$ pC/N, $k_p\sim47.6\%$, $\varepsilon_r\sim4638$, and tan $\delta\sim0.015$ when sintered at a low temperature of ~1400 °C. As a result, the BCTZ-*x*Pr ceramic is a promising candidate for lead-free piezoelectric ceramics.

Keywords: Lead-free ceramics; $(Ba,Ca)(Ti,Zr)O_3$; Piezoelectric properties

1. Introduction

Lead-free piezoelectric materials are promising as the candidate materials for buzzers, transducers, and piezoelectric transformers because of their high piezoelectric properties and environmental friendliness [1–4]. Considerable attention has been given to $K_{0.50}Na_{0.50}NbO_3$, $Bi_{0.5}Na_{0.5}TiO_3$, and $BiFeO_3$ materials [1,2,5–16], but their piezoelectric behavior is inferior to that of $Pb(Zr,Ti)O_3$ (PZT) ceramics [17]. Recently, a high piezoelectric constant (d_{33}) has been well demonstrated in $(Ba,Ca)(Ti,Zr)O_3$ (BCTZ) ceramics by constructing a tricritical point at room temperature [3,18,19].

A high d_{33} value of BCTZ ceramics could be induced by constructing a phase transition at/near room temperature [3,19]. Enhanced piezoelectric properties could be attributed to the involvement of a tricritical point at/near room temperature [3,18,19]. However, such a phase transition results in a strong temperature dependence of piezoelectric properties, which limits its practical application [3,18,19]. Some attempts have been conducted to improve the temperature stability of BCTZ ceramics by shifting the phase boundary to below room temperature, but their piezoelectric properties are still not ideal [20–22]. As a result, the improvement of the temperature stability and piezoelectric properties of BCTZ ceramics becomes a tough issue for the practical application. Moreover, such a high d_{33} value of BCTZ ceramics could be obtained only by a high processing temperature of >1500 °C [3,19]. Some methods have been used to decrease the sintering temperature of BCTZ ceramics [23,24], and unfortunately their d_{33} value often drops dramatically to below 400 pC/N [23,24].

Our objective of this work is to decrease the sintering temperature of BCTZ ceramics without affecting negatively the piezoelectric constant, and the Pr_2O_3 is used to modify the BCTZ lead-free piezoelectric ceramics. The effect of Pr_2O_3 content on the microstructure and piezoelectric properties of BCTZ ceramics is also investigated, and the underlying physical mechanisms are addressed.

2. Experimental procedure

$(Ba_{0.85}Ca_{0.15})(Ti_{0.90}Zr_{0.10})O_3-x$ wt% Pr_2O_3 (BCTZ-*x*Pr) ($x=0$, 0.02, 0.04, 0.06, 0.08, 0.10, 0.15, and 0.20) ceramics

*Corresponding author.
E-mail addresses: wujiagang0208@163.com, sewujg@scu.edu.cn (J. Wu).

0272-8842/$36.00
http://dx.doi.org/10.1016/j.ceramint.2012.05.008

were prepared by the conventional solid-state method. In this work, raw materials were $BaCO_3$ (99.9%), $CaCO_3$ (99%), TiO_2 (98%), ZrO_2 (99%), and Pr_2O_3 (99.99%), proved by Sinopharm Chemical Reagent Co., Ltd. All raw materials were weighed according to the formula of $(Ba_{0.85}Ca_{0.15})(Ti_{0.90}Zr_{0.10})O_3 - x$ wt% Pr_2O_3, and then these powders were ball milled for 24 h with agate ball media and alcohol. After calcination at 1200 °C for 2 h, calcined powders were milled again for 12 h, and pressed into the disks of ~1.0 cm diameter and ~1.0 mm thickness under 10 MPa using PVA as a binder. After burning off PVA, these pellets were sintered at 1350–1400 °C for 3 h in air. Silver paste was sintered on both sides of samples at ~700 °C for 10 min to form the electrodes for their electrical measurements. These ceramics were poled in a room-temperature silicon oil bath by applying the *dc* electric fields of 4 kV/mm for 30 min. All measurement of electrical properties was conducted after 24 h.

The phase structure of these ceramics was analyzed by using X-ray diffraction (XRD, Rigaku, Japan). Scanning electron microscopy (SEM) was employed to study the surface morphology of these ceramics. The d_{33} value of these ceramics was measured by using a piezo-d_{33} meter (ZJ-3A, China). Their room-temperature dielectric properties and dielectric behavior as a function of measurement temperatures was obtained by using an *LCR* meter (HP 4980, Agilent, U.S.A.). Ferroelectric properties of these ceramics were characterized by using the Radiant precise workstation (Radiant Technologies, Medina, NY).

3. Results and discussion

Fig. 1(a) shows the XRD patterns of Pr_2O_3-modified BCTZ ceramics. These ceramics with $x < 0.08$ wt% have a pure structure, and secondary phases gradually form with increasing Pr_2O_3 contents ($x \geq 0.08$ wt%). Moreover, all ceramics have a tetragonal phase regardless of Pr_2O_3 contents. Therefore, the introduction of Pr_2O_3 cannot change the crystal structure of BCTZ ceramics. The position of diffraction peaks of Pr_2O_3-doped BCTZ ceramics with $x \leq 0.04$ wt% shifts to a high angle because of the Pr substitution for the (Ti, Zr) site, confirming the Pr partly enters into the lattice of BCTZ ceramics. However, the XRD peak position almost keeps unchanged with further increasing Pr_2O_3 contents from 0.06 to 0.20 wt%, and some secondary phases are observed in these ceramics with $x \geq 0.08$ wt%. To further confirm the phase structure of Pr_2O_3-modified BCTZ ceramics, their Raman spectra was measured in the region of 100–1000 cm^{-1}, as shown in Fig. 2. These modes consist of the longitudinal (LO) and transverse (TO) components because of the long electrostatic force [25]. Raman modes are assigned to be $A_1(TO_1)$, $A_1(TO_2)$, $E(TO_2)$, $E(TO_2)$, $A_1(TO_3)$, and $A_1(LO_3)/E(LO_3)$. The tetragonal structure of $BaTiO_3$-based materials could be confirmed by the $E(TO_2)$ phonon mode [26]. Therefore, the micro-Raman scattering spectra further conforms the formation of a tetragonal structure in these ceramics.

Fig. 3(a) and (b) shows the surface morphologies of Pr_2O_3-modified BCTZ ceramics with $x=0$ and 0.06 wt%. The average grain size of Pr_2O_3-modified BCTZ ceramics slightly increases with the introduction of Pr_2O_3 contents. The Pr^{3+} substitution for (Ti, Zr)$^{4+}$ leads to the generation of oxygen vacancies, and then these oxygen vacancies can enhance the mass transfer and improve the grain growth, finally resulting in the increase of the grain size. Moreover, the undoped BCTZ ceramic has a lower density than that of Pr_2O_3-modified BCTZ ceramics with $x=0.06$ wt%, as shown in Fig. 3. As a result, the addition of Pr_2O_3 could effectively promote the densification of BCTZ ceramics.

Fig. 4(a) and (b) show the temperature dependence of the dielectric behavior of Pr_2O_3-modified BCTZ ceramics, measured at 1–100 kHz. All ceramics only exhibit a tetragonal-cubic phase transition (T_c) in the range of measurement temperatures from 20 to 200 °C, and the coexistence of two phases cannot be observed, confirming the involvement of a tetragonal phase in these ceramics. It is also observed from Fig. 4(a) and (b) that the T_c value of these ceramics slightly decreases with the introduction of

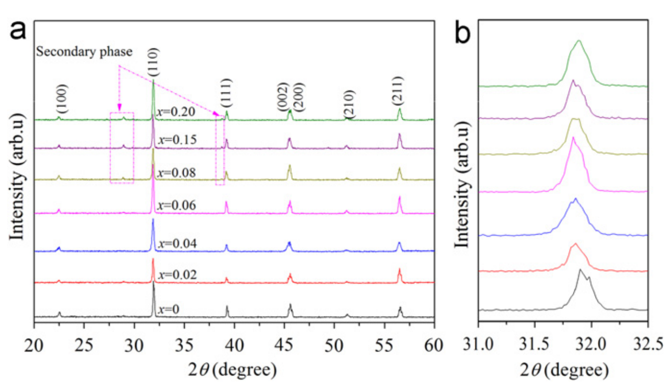

Fig. 1. (a) XRD patterns and (b) expanded XRD patterns of Pr_2O_3-doped BCZT ceramics at $x=0$–0.20 wt%.

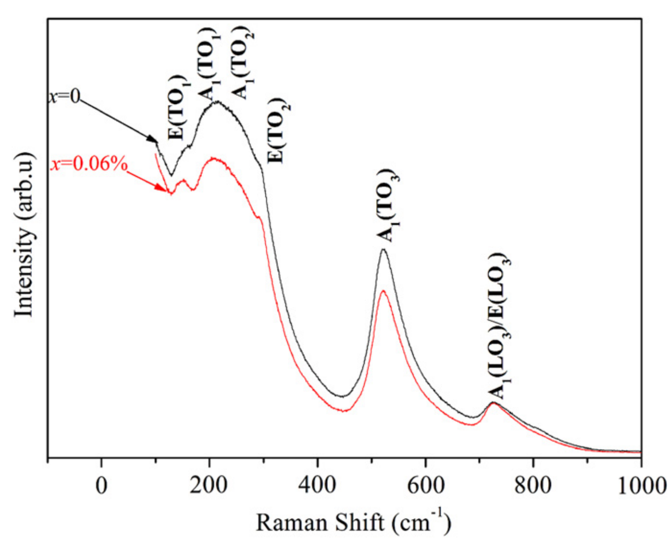

Fig. 2. Raman spectrum of Pr_2O_3-doped BCZT ceramics with $x=0$ and 0.06 wt%.

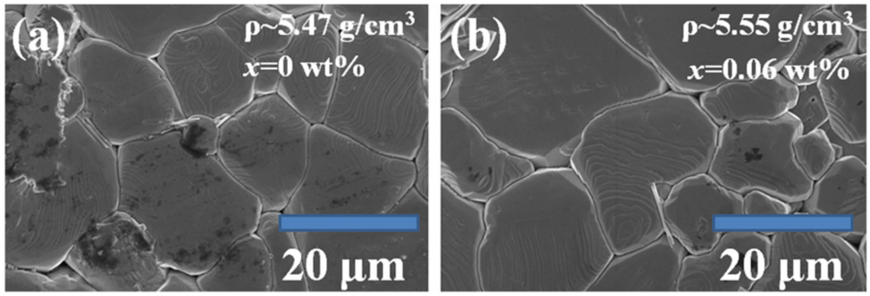

Fig. 3. SEM morphologies of Pr_2O_3-doped BCZT ceramics with (a) $x=0$ and (b) 0.06 wt%.

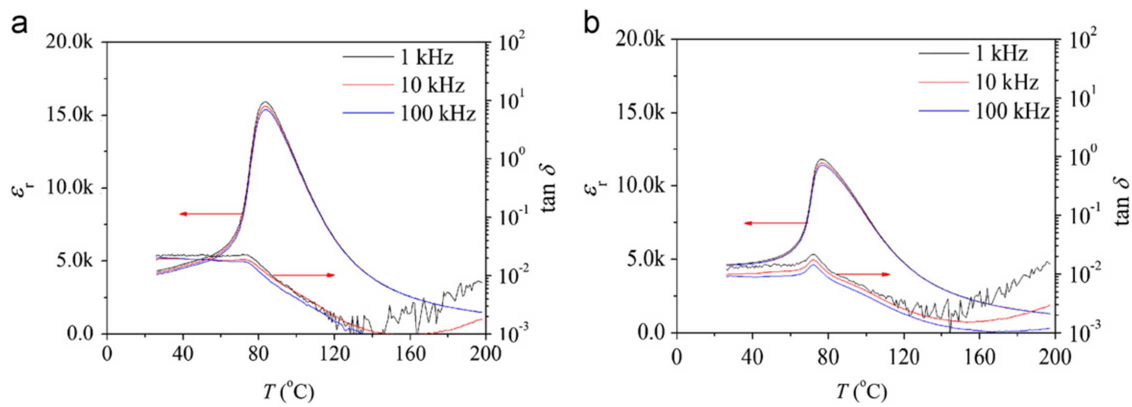

Fig. 4. Temperature-dependent dielectric properties of Pr_2O_3-modified BCTZ ceramics with (a) $x=0$ and (b) $x=0.06$ wt%.

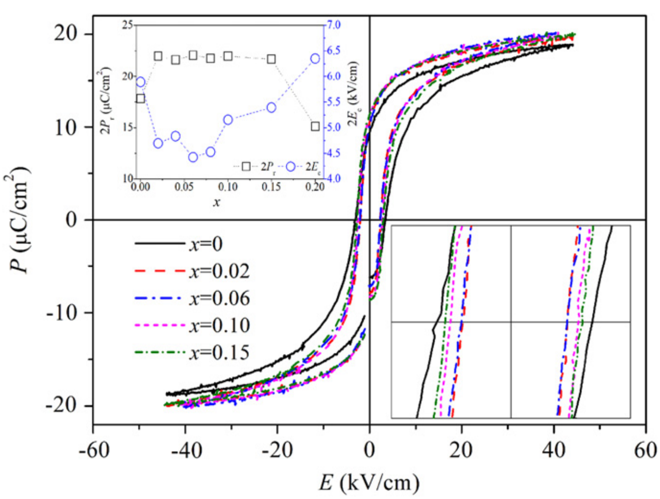

Fig. 5. *P–E* loops of BCTZ ceramics with different Pr_2O_3 contents, where the inserts are $2P_r$ and $2E_c$ values as a function of x and enlarged *P–E* loops.

Pr_2O_3 because of the addition of Pr [27], and a lower dielectric loss is demonstrated in Pr_2O_3-modified BCTZ ceramics [27].

Fig. 5 shows the *P–E* loops of BCTZ ceramics with different Pr_2O_3 contents, measured at 10 Hz and room temperature. All ceramics exhibit a saturated *P–E* loop regardless of Pr_2O_3 content. The insert of Fig. 5 plots the $2P_r$ and $2E_c$ values of BCTZ-xPr ceramic as a function of x. The $2P_r$ value dramatically increases with increasing x contents, almost keeps unchanged in the range of $0.02 \le x \le 0.15$, and then decreases with further increasing x contents because of the formation of some secondary phases. However, the E_c gradually drops, reaches a minimum value at $x=0.06$, and then increases with further increasing x contents because of more defects induced by excessive Pr_2O_3 contents. Moreover, enlarged *P–E* loops also confirm the change of E_c values, as shown in the insert of Fig. 5. As a result, the ceramic with $x=0.06$ wt% has an optimum ferroelectric behavior of $2P_r \sim 22.1\ \mu C/cm^2$ and $2E_c \sim 4.43$ kV/cm. These results clearly indicate that Pr_2O_3-doped BCTZ ceramics have an advantage for a low-voltage-operating ferroelectric memory material, and similar phenomenon is also observed in Pr-doped $SrBi_2Ta_2O_9$ ceramics [27].

Fig. 6(a) plots the dielectric constant (ε_r) and dielectric loss (tan δ) of BCTZ ceramics with different Pr_2O_3 contents, measured at 1 kHz and room temperature. The ε_r value is almost a constant in the range of ≤ 0.15 wt%, and then dramatically drops at $x=0.20$ wt% because of the formation of secondary phases, as shown in Fig. 1. Moreover, Pr_2O_3-modified BCTZ ceramics have a low tan δ value of 0.014–0.020 regardless of Pr_2O_3 contents [27]. Fig 6(b) plots the d_{33} and k_p values of BCTZ ceramics with different Pr_2O_3 contents, measured at room temperature. The d_{33} value gradually increases, reaches a maximum at $x=0.06$ wt%, and then drops with increasing x contents.

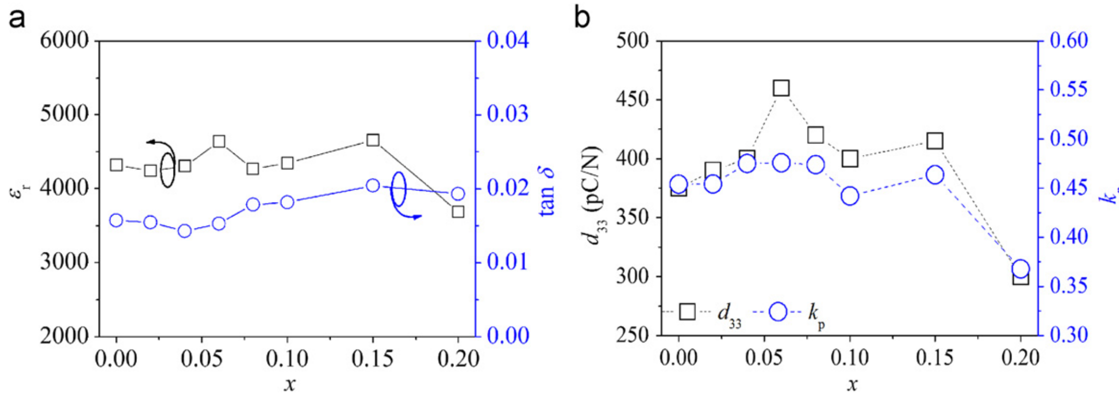

Fig. 6. (a) Dielectric behavior and (b) piezoelectric properties of BCTZ ceramics with different Pr_2O_3 contents.

Similarity to the change of d_{33} value, the k_p value also gets a maximum at $x=0.06$ wt%. As a result, the ceramic with $x=0.06$ wt% has an enhanced piezoelectric behavior of $d_{33}\sim460$ pC/N and $k_p\sim47.6\%$ because of the introduction of optimum Pr_2O_3 contents. In this work, the d_{33} value of Pr_2O_3-modified BCTZ ceramicsis much higher than those reported results of BCTZ ceramics [20–23].

4. Conclusions

Pr_2O_3-doped $Ba_{0.85}Ca_{0.15}Ti_{0.90}Zr_{0.10}O_3$ (BCTZ-xPr) ceramics were prepared by the conventional solid-state method. These ceramics have a pure tetragonal phase in the limited range of <0.08 wt%, and the sintering temperature decreases to 1400 °C by the introduction of Pr_2O_3 to BCTZ. An enhanced electrical behavior of $d_{33}\sim460$ pC/N, $k_p\sim47.6\%$, $\varepsilon_r\sim4638$, and tan $\delta\sim0.015$ is observed in the ceramic with $x=0.06$ wt%. As a result, the BCTZ ceramic with optimum Pr_2O_3 contents is a promising candidate for lead-free piezoelectric ceramics.

Acknowledgements

Authors gratefully acknowledge the supports of the National Science Foundation of China(NSFC Nos. 51102173, 50772068 and 50972001), the Fundamental Research Funds for the Central Universities (2012SCU04A01), and the introduction of talent start funds of Sichuan University (2082204144033).

References

[1] Y. Saito, H. Takao, T. Tani, T. Nonoyama, K. Takatori, T. Homma, T. Nagaya, M. Nakamura, Lead-free piezoceramic, Nature 432 (2004) 84–87.
[2] S.J. Zhang, R. Xia, T.R. Shrout, Modified $(K_{0.5}Na_{0.5})NbO_3$ based lead-free piezoelectrics with broad temperature usage range, Applied Physics Letters 91 (2007) 132913.
[3] W.F. Liu, X.B. Ren, Large piezoelectric effect in Pb-Free ceramics, Physical Review Letters 103 (2009) 257602.
[4] D. Damjanovic, A morphotropic phase boundary system based on polarization rotation and polarization extension, Applied Physics Letters 97 (2010) 062906.
[5] J.G. Wu, D.Q. Xiao, Y.Y. Wang, W.J. Wu, B. Zhang, J. Li, J.G. Zhu, $CaTiO_3$-modified $[(K_{0.5}Na_{0.5})_{0.94}Li_{0.06}](Nb_{0.94}Sb)O_3$ lead-free piezoelectric ceramics with improved temperature stability, Scripta Materialia 59 (2008) 750–752.
[6] Y. Guo, K. Kakimoto, H. Ohsato, Phase transitional behavior and piezoelectric properties of $(Na_{0.5}K_{0.5})NbO_3$–$LiNbO_3$ ceramics, Applied Physics Letters 85 (2004) 4121–4123.
[7] R.Z. Zuo, X.S. Fang, C. Ye, Phase structures and electrical properties of new lead free $(Na_{0.5}K_{0.5})NbO_3$–$(Bi_{0.5}Na_{0.5})TiO_3$ ceramics, Applied Physics Letters 90 (2007) 092904.
[8] H.L. Du, W.C. Zhou, F. Luo, D.M. Zhu, S.B. Qu, Z.B. Pei, Perovskite lithium and bismuth modified potassium-sodium niobium lead-free ceramics for high temperature applications, Applied Physics Letters 91 (2007) 182909.
[9] J. Rödel, W. Jo, K. Seifert, E.M. Anton, T. Granzow, Perspective on the development of lead-free piezoceramics, Journal of the American Ceramic Society 92 (2009) 1153–1177.
[10] Y. Chang, Z. Yang, L. Wei, Microstructure, density, and dielectric properties of lead-free $(K_{0.44}Na_{0.52}Li_{0.04})(Nb_{0.96-x}Ta_xSb_{0.04})O_3$ Piezoelectric Ceramics, Journal of the American Ceramic Society 90 (2007) 1656–1658.
[11] D. Lin, K.W. Kwok, H.L.W. Chan, Structure and electrical properties of $Bi_{0.5}Na_{0.5}TiO_3$–$BaTiO_3$–$Bi_{0.5}Li_{0.5}TiO_3$ lead-free piezoelectric ceramics, Solid State Ionics 178 (2008) 1930–1937.
[12] D. Lin, D. Xiao, J. Zhu, P. Yu, Piezoelectric and ferroelectric properties of $[Bi_{0.5}(Na_{1-x-y}K_xLi_y)_{0.5}]TiO_3$ lead-free piezoelectric ceramics, Applied Physics Letters 88 (2006) 062901.
[13] Y. Hiruma, R. Aoyagi, H. Nagata, T. Takenaka, Ferroelectric and piezoelectric properties of $(Bi_{1/2}K_{1/2})TiO_3$ ceramics, Japanese Journal of Applied Physics 44 (2005) 5040–5044.
[14] F. Yan, S. Miao, I. Sterianou, I.M. Reaney, M.O. Lai, L. Lu, W.D. Song., Multiferroic properties and temperature-dependent leakage mechanism of Sc-substituted bismuth ferrite-lead titanate thin films, Scripta Materialia 64 (2011) 458–461.
[15] F. Yan, M.O. Lai, L. Lu, T.J. Zhu., Enhanced multiferroic properties and valence effect of Ru-doped $BiFeO_3$ thin films, Journal of Physical Chemistry C 114 (2010) 6994–6998.
[16] F. Yan, I. Sterianou, S. Miao, I.M. Reaney, M.O. Lai, L. Lu, Magnetic, ferroelectric, and dielectric properties of $Bi(Sc_{0.5}Fe_{0.5})O_3$–$PbTiO_3$ thin films, Journal of Applied Physics 105 (2009) 074101.
[17] B. Jaff, W.R. Cook, H. Jaffe, Piezoelectric Ceramics, Academics Press, New York, 1971, pp. 115–181.
[18] J. Wu, D. Xiao, W. Wu, Q. Chen, J. Zhu, Z. Yang, J. Wang, Role of room-temperature phase transition in the electrical properties of (Ba, Ca)(Ti, Zr)O_3 ceramics, Scripta Materialia 65 (2011) 771–774.

[19] P. Wang, Y. Li, Y. Lu, Enhanced piezoelectric properties of $(Ba_{0.85}Ca_{0.15})(Ti_{0.9}Zr_{0.1})O_3$ lead-free ceramics by optimizing calcination and sintering temperature, Journal of the European Ceramic Society 31 (2011) 2005–2012.

[20] W. Li, Z. Xu, R. Chu, P. Fu, P. An, Effect of Ho Doping on Piezoelectric Properties of BCZT ceramics, Ceram. Inter. http://dx.doi.org/10.1016/j.ceramint.2011.12.066.

[21] W. Li, J. Hao, W. Bai, Z. Xu, R. Chu, J. Zhai, "Enhancement of the Temperature Stabilities in Yttrium Doped (Ba0.99Ca0.01)(Ti0.98Zr0.02)O3 ceramics", J. Alloys Compd., http://dx.doi.org/10.1016/j.jallcom.2012.03.110.

[22] J. Wu, W. Wu, D. Xiao, J. Wang, Z. Yang, Z. Peng, Q. Chen, J. Zhu, (Ba, Ca)(Ti, Zr)O_3–$BiFeO_3$ lead-free piezoelectric ceramics, Current Applied Physics 12 (2012) 534–538.

[23] T. Chen, T. Zhang, G. Wang, J. Zhou, J. Zhang, Y. Liu, Effect of CuO on the microstructure and electrical properties of $Ba_{0.85}Ca_{0.15}Ti_{0.90}Zr_{0.10}O_3$ piezoceramics, Journal of Materials Science 47 (2012) 4612–4619.

[24] W. Li, Z. Xu, R. Chu, P. Fu, G. Zang, High piezoelectric d_{33} coefficient of lead-free $(Ba_{0.93}Ca_{0.07})(Ti_{0.95}Zr_{0.05})O_3$ ceramics sintered at optimal temperature, Materials Science and Engineering B 176 (2011) 65–67.

[25] P.S. Dobal, R.S. Katiyar, Studies on ferroelectric perovskites and Bi-layered compounds using micro-Raman spectroscopy, Journal of Raman Specroscopy 33 (2002) 405–423.

[26] B.D. Begg, S. Kim, Finnie, E.R. Vance, Raman study of the relationship between room-temperature tetragonality and the curie point of barium titanate, Journal of the American Ceramic Society 79 (1996) 2666–2672.

[27] M. Miyayama, Y. Noguchi, Polarization properties and oxygen-vacancy distribution of $SrBi_2Ta_2O_9$ ceramics modified by Ce and Pr, Journal of the European Ceramic Society 25 (2005) 2477–2482.